Mathematical Biosciences 300 (2018) 157–167

Contents lists available at ScienceDirect

Mathematical Biosciences

journal homepage: www.elsevier.com/locate/mbs

# Age-structure density-dependent fertility and individuals dispersal in a population model

M. Marvá*, F. San Segundo

*U. D. Matemáticas, Universidad de Alcalá, Alcalá de Henares 28871, Spain*

ARTICLE INFO

*Keywords:*
Leslie model
Density-dependent fertility
Dispersal
Approximate aggregation methods

ABSTRACT

In this work, we analyze the interplay between general age structured density-dependent fertility functions and age classes dispersal in a patchy environment. As novelties, (i) the fertility function depends on age classes (instead of on the total population size) and (ii) dispersal patterns are also allowed to be different for individuals belonging to different age classes.

Our results highlight the interplay between the shape of the age structured density-dependent fertility function and the age classes dispersal patterns. We analyze this interaction from an environmental management point of view by exploring the consequences of connecting patches that can sustain a population (source patch) or cannot (sink patch), as well as its relation to component Allee effects and strong Allee effects.

In particular, we have found scenarios such that the metapopulation goes extinct when two isolated source patches are connect due to heterogeneous age classes distribution. On the contrary, there are settings such that heterogeneous age classes distribution enables two isolated sink patches to be sustainable when connected. Besides, we discuss what kind of local interventions are helpful to manage component Allee effect and its impact at the metopopulation level.

The source code used to simulations is fully available. The code is presented as a knitr reproducible document in the open source R computing system. Thus, free access and usability of the code are granted.

## 1. Introduction

A key process in the survival of an age structured population is the way new reproductive individuals are incorporated to the community. Adult reproductive individuals die sooner or later, and the replacement/renewal strategy is crucial in order to keep the fitness of the population.

There is a wide range of mechanisms either pushing juvenile and adult individuals to remain together or leading them to occupy mostly separated areas. For instance, in small mammals ecology the usual assumption is that adults follow juveniles when they disperse [41]. On the other hand, juveniles dispersal (away from adults) is a mechanism to avoid consanguinity by inbreeding with close relatives [17], competition for resources or mating due to density-dependent effects [21]. Indeed, it is broadly recognized that many vital rates are density-dependent [8,28], as the fertility rate [11,12]. A particular (but very important) case [10] is that of *component Allee effects* that, following [12], are density-dependent parameters of the model with positive feedback effects at low population density. That is to say that at low population density the fitness of the population worsens as the population density decreases. If the weight on the model of this component is “strong” enough, it can lead to the existence of a population threshold below which a population would go extinct.

Apart from these density-dependent dispersal drivers, it is accepted that human activity plays an important role in populations dispersal regardless of being intentional [20] or a side effect [21].

This work deals with an age structured population inhabiting a patchy environment and we analyze the effect of age classes dispersal among patches for different density-dependent fertility functions [11] that may include component Allee effects. The novelties consist of:

1. Generalize those fertility functions presented in [38,39] by introducing age structure.
2. Let individuals of each age class to disperse in an independent way [1].

We assume that both maturation and dispersal processes are completed in the time elapsed between two reproduction periods [4]. In particular, it means that the dispersal process is at equilibrium before the next reproduction period takes place (see Section 2 for further

* Corresponding author.
*E-mail addresses:* marcos.marva@uah.es (M. Marvá), fernando.sansegundo@gmail.com (F. San Segundo).

https://doi.org/10.1016/j.mbs.2018.03.029
Received 31 May 2017; Received in revised form 20 February 2018; Accepted 29 March 2018
Available online 30 March 2018
0025-5564/ 

details). In other words, dispersal and demography events take place at different time scales [4,27,36]. Understanding how ecological phenomena interact across temporal scales is important in theoretical ecology [22,25], since it is known that differences in process time scales may be critical for system dynamical behavior [22,24,26].

We analyze the aforementioned two time scales system using approximate aggregation techniques [5] and bifurcation techniques for Leslie-like nonlinear matrices [11]. There are other works considering both dispersal (that requires of spatial structure) and age structure, even considering time scales, as [29,37], that, nevertheless, do not consider age structured density-dependent fertility functions nor the consequences of different dispersal schemes.

Our results highlight the key role of age classes dispersal and age classes density-dependent fertility in the global dynamics of populations inhabiting fragmented habitats. It turns out that the dynamics of a spatially distributed age structured population can be sensitive not only to whether juvenile and adult individuals remain together in a given patch (increasing population density there) or occupy mostly separated regions, but also to whether the age classes structure is homogeneous (similar proportion of individuals of both age classes at each patch) or heterogeneous.

We relate these features with two popular management tools in the design of species conservation or species control strategies: the construction of corridors between patches allowing individuals to disperse [15,32] and the implementation of refuges, artificial habitats or protected areas [6,31,40]. In particular, we have found conditions that lead to population extinction (respectively, survival) in source-source patches (respectively, in sink–sink patches) such that the contrary outcome would happen if the populations in the patches had remained isolated. These apparently counterintuitive results are explained in terms of heterogeneous age classes distribution between patches.

Furthermore, our results point out that, if not all the patches present component Allee effects, there exist dispersal rates that either "silence" the component Allee effects or enhance them so that an Allee population threshold appears for the entire population. This findings may help environment managers to determine what interventions are the appropriate ones (and which are ineffective) to control the population dynamics.

Part of our results are illustrated through simulations, and the source code to compute bifurcation diagrams and other simulations at [16]. The code is presented as a knitr [42] reproducible document available from an open GitHub repository [16] in the open source R computing system [30]. In particular, this feature allows other researchers to reproduce our simulations or to perform simulations of their interest and not covered in the manuscript.

This work is organized as follows. In Section 2, we build up the model upon a slow-fast system and we apply the aforementioned dimension reduction techniques to derive the reduced system. In Section 3, we analyze the original model through the reduced system aided by bifurcation techniques. Section 4 is devoted to the discussion of results. Appendix A contains technical details on the dimension reduction process (Appendix A.1) and the derivation of the main bifurcation parameter (Appendix A.2).

## 2. Presentation of the model

We consider an age structured population with two age classes: juvenile (immature) and adult (mature) individuals. The population is further assumed to inhabit a fragmented habitat consisting of $N$ patches, and individuals are allowed to move between patches. We denote $J_i$ and $A_i$, respectively, the densities of juveniles and adults in patch $i = 1, ...,N$. The population vector is

$$\overrightarrow{N} = (J_1,...,J_N, A_1,...,A_N)^T,$$

where $T$ denotes transposition. We also use the following notation

$$J = \sum_{i=1}^{N} J_i, \qquad A = \sum_{i=1}^{N} A_i, \qquad \overrightarrow{n} = (J, A)^T,$$

for the total number of juvenile and adult individuals. We denote $\overline{\mathbb{R}}^m_+$ the non negative cone and $\mathbb{R}^m_+$ stands for the positive cone in $\mathbb{R}^m$.

In the sequel, we describe the two processes involved in the model: demography and dispersal.

### 2.1. Slow process: demography

Demography is described by means of a density-dependent Leslie matrix. On the one hand, let $\sigma_i^J$ and $\sigma_i^A$ be the constant fraction of the juveniles and adults in patch $i = 1, ...,N$ alive at time $t$ that survive to time $t + 1$. The survival rates, $\sigma_i^J$ and $\sigma_i^A$ lie between 0 and 1.

On the other hand, let $\phi_i(J_i, A_i)$ be the number of juveniles at time $t + 1$ produced by an adult at time $t$ in patch $i = 1, ...,N$. We assume that $\phi_i$ depends on the population structure, juveniles and adults, in the corresponding patch. The fertility functions are strictly positive, $\phi_i(0, 0) > 0$ and $\lim_{\|(J_i,A_i)\|\to\infty}\phi_i(J_i, A_i) = 0$. The usual assumption when the fertility function $\phi_i$ depends on the total population is that it is either strictly decreasing [38,43] or unimodal [39]. Keeping this features in mind and taking into account that the age structure of the population allows the fertility function to depend on $J$ and $A$, we consider three basic shapes that generalize those presented in [38,39]:

- We say that $\phi(J, A)$ is of class C1 if there is negative feedback on $J$ and $A$, what is to say that it is strictly decreasing with respect both variables, as in the left panel of Fig. 1. The fertility decreases as the number of juvenile/adult individuals increases due to competition for resources [10].
- We say that $\phi(J, A)$ is of class C2 if it is an unimodal function [39] in both variables, as in the surface in the center panel of Fig. 1 (see also [7]). In this case, there is negative feedback at high population

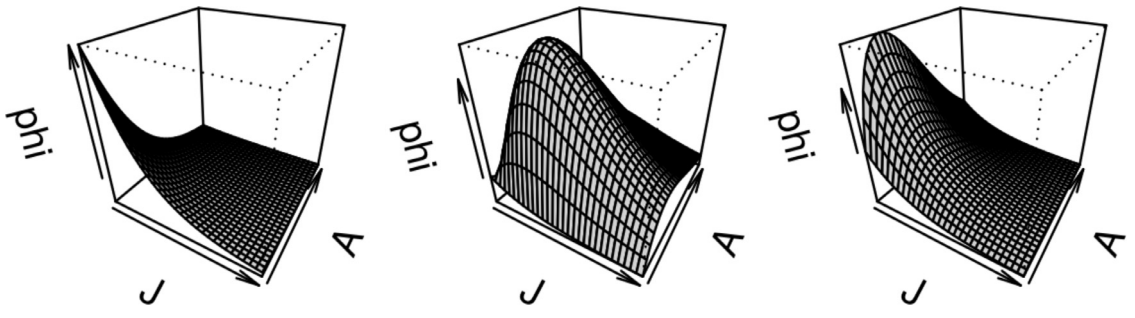


**Fig. 1.** Shapes of the fertility functions considered. We will use these precise expressions for simulations throughout the manuscript. Left: class C1, strictly decreasing with respect to both variables, $\phi(J, A) = \psi \exp(-a_J J_1 + a_A A_1))$. Center: class C2, unimodal with respect to both variables, $\phi(J, A) = \psi\cdot(1 + JA)\exp(-a_J J - a_A A))$. Right: class C3, strictly decreasing with respect to the number of juveniles and unimodal with respect to the number of adult individuals, $\phi(J, A) = \psi\cdot(1 + A)\exp(-a_J J - a_A A))$. In all figures $\psi = 50$, $a_J = a_A = 0.085$, $0 \le J, A \le 50$.

densities (as for class C1) and there is positive feedback at low population densities, i.e. the fertility rate decreases as the number of either juvenile or adult individuals decreases. For instance, regarding adults, in sexual reproduction, low densities of adult individuals implies difficulties to find mates, or a reduction on pollination effectiveness due to low plant population density [10]. On the other hand, when juveniles contribute to the welfare of the population (foraging efficiency, helper role in obligate cooperative breeders, surveillance tasks,...) at low population densities a decrease in the number of juveniles may entail a worsening of the population's fitness by lowering fertility (and/or survival) rate (see [10, Table 2.1] and references therein).

- A new class *C*3 can be considered. Namely, $\phi_i$ is strictly decreasing with respect $J$ and unimodal on $A$. This can occur if a large number of juveniles requires a large number of adults dedicated to parental tasks and not available for reproduction. Besides, the function is unimodal with respect to $A$ because of the reasons described before. The surface in the right panel of Fig. 1 displays this feature.

Finally, some regularity will be needed for the mathematical analysis, so that we ask $\phi_i \in C^1(\overline{\mathbb{R}}^2_+, \mathbb{R}_+)$, for $i = 1, 2, 3$.

The demography is described thus by the map $\overrightarrow{N} \mapsto \mathscr{S}(\overrightarrow{N})\cdot\overrightarrow{N}$ where $\mathscr{S}(\overrightarrow{N})$ is the following density-dependent Leslie-like matrix

$$\mathscr{S}(\overrightarrow{N}) = \begin{pmatrix} 0 & \phi(\overrightarrow{N}) \\ 0ex3ex\Sigma_J & \Sigma_A \end{pmatrix}$$

and $\phi$, $\Sigma_J$ and $\Sigma_A$ are diagonal matrices of dimension $N \times N$ as follows: $\phi(\overrightarrow{N}) = \mathrm{diag}(\phi_1(J_1, A_1), ..., \phi_N(J_N, A_N))$, $\Sigma_J = \mathrm{diag}(\sigma_1^J, ..., \sigma_N^J)$, $\Sigma_A = \mathrm{diag}(\sigma_1^A, ..., \sigma_N^A)$. Therefore, demography dynamics is defined by

$$\overrightarrow{N}(t+1) = \mathscr{S}(\overrightarrow{N}(t))\overrightarrow{N}(t)$$

where $t$ is the maturation time. We use capital calligraphic letters to denote matrices all along the manuscript.

### 2.2. Fast process: dispersal

Juvenile and adult dispersal rates are supposed to be constant and are represented by stochastic matrices

$$\mathscr{F}_J = \begin{pmatrix} p_{11}^J & \cdots & p_{1N}^J \\ \cdots & \cdots & \cdots \\ p_{N1}^J & \cdots & p_{NN}^J \end{pmatrix}, \qquad \mathscr{F}_A = \begin{pmatrix} p_{11}^A & \cdots & p_{1N}^A \\ \cdots & \cdots & \cdots \\ p_{N1}^A & \cdots & p_{NN}^A \end{pmatrix},$$

where $0 < p_{ij}^\theta < 1$ stands for the fraction of individuals of class $\theta = J, A$ leaving patch $j$ towards patch $i$, $i \neq j$ and $p_{ii}^\theta$ stands for the fraction of individuals that remain at patch $i$. Therefore, dispersal is given by the map $\overrightarrow{N} \mapsto \mathscr{F}\overrightarrow{N}$ where $\mathscr{F} = \mathrm{diag}(\mathscr{F}_J, \mathscr{F}_A)$ is a block diagonal matrix and and the dispersion process is defined by

$$\overrightarrow{N}(\hat{t}+1) = \mathscr{F}\overrightarrow{N}(\hat{t})$$

where $\hat{t}$ stands for the time elapsed for each dispersal event, that is supposed to be much sorter that the maduration time $t$.

### 2.3. The complete system

We build up now the so called complete model combining the two processes presented in Sections 2.1 and 2.2. We assume that all juveniles either die or mature becoming adults [4,11] and reproduction takes place once within each unit of time $t$. Dispersal events are considered to be much more frequent that demographic processes, so that we consider them acting at different time scales [4,36]. We must choose the time unit for the model as the time unit associated to each process are supposed to be quite different. If we choose the faster one, only a "fraction" of the demographic process would take places within each time unit, what makes no sense. Thus, we choose the unit of time $t$ of the slow process (demography) for the model, so that several dispersal events, lets say $k$, take place between $t$ and $t+1$. By reasoning sequentially we let $\mathscr{F}$ act $k$ times, $\mathscr{F}^k$, followed by $\mathscr{S}$, obtaining a two time scales difference equations system of the general form [34]

$$\overrightarrow{N}(t+1) = \mathscr{S}(\mathscr{F}^k\overrightarrow{N}(t))\mathscr{F}^k\overrightarrow{N}(t) \tag{1}$$

Note that, even when considering just two patches, it may be complicated, unfeasible or useless to get an explicit expression for the equation system , and things get worse and worse as the number of patches increases. Hopefully, such a difficulty can be overcome by assuming that the ratio between unit time is large enough.

### 2.4. Approximate aggregation of system (1)

In this section we sketch a procedure (see Appendix A.1. or [34] for details) that allows to analyze system (1) by means of a lower dimensional system for large enough values of $k$. The fast process is described by means of a regular stochastic matrix, and the Perron Frobenius theorem [35] guarantees the existence of the limit

$$\lim_{k\to\infty}\mathscr{F}^k = \overline{\mathscr{F}}.$$

It means that the spatial distribution of juvenile and adult individuals reaches an equilibrium, denoted by $\mu_J$ and $\mu_A$. Namely,

$$\mu_\theta = (\mu_1^\theta, ..., \mu_N^\theta) \tag{2}$$

where $\mu_i^\theta$ stands for the fraction of individuals of age class $\theta \in \{J, A\}$ at patch $i = 1, ..., N$. Let us recall that $(\mu_J, \mu_A)$ is the solution of the linear equations system $\mathscr{F}\overrightarrow{X} = \overrightarrow{X}$, $\sum_{i=1}^N X_i = 1$. Besides, we use such a limit to build up the *auxiliary system*, that does not depend on $k$,

$$\overrightarrow{N}(t+1) = \mathscr{S}(\overline{\mathscr{F}}\overrightarrow{N}(t))\overline{\mathscr{F}}\overrightarrow{N}(t) \tag{3}$$

The relation between systems (1) and (3) is fully described in [34]. Furthermore, following [34] (see Appendix A.1 here) yields the so called *aggregated system* (see (16)):

$$\overrightarrow{n}(t+1) = \begin{pmatrix} 0 & \overline{\phi}(\overrightarrow{n}(t)) \\ 0ex3ex\overline{\sigma}_J & \overline{\sigma}_A \end{pmatrix}\overrightarrow{n}(t) = \mathscr{L}(\overrightarrow{n}(t))\overrightarrow{n}(t) \tag{4}$$

where

$$\overline{\phi}(J, A) = \sum_{i=1}^N \mu_i^A\phi_1(\mu_i^J J, \mu_i^A A), \qquad \overline{\sigma}_J = \sum_{i=1}^N \mu_i^J\sigma_1^J, \qquad \overline{\sigma}_A = \sum_{i=1}^N \mu_i^A\sigma_1^A. \tag{5}$$

Note that the entries of matrix $\mathscr{L}(\overrightarrow{n})$ are a sort of average of the components of the local dynamics weighted by the asymptotic spatial distribution of the individuals of each age class.

The following result, that is a restatement of one of the main results in [34] describes the relation between the complete (1), the auxiliary (3) and the reduced (4) systems.

**Theorem 2.1.** *Consider system (1) and let be a hyperbolic equilibrium point of the aggregated system (4). Then*

$$\overrightarrow{N}^* = (\mu_J J^*, \mu_A A^*)^T \in \mathbb{R}^{2N}$$

*is a hyperbolic equilibrium point of system (3) with the same stability properties as $\overrightarrow{n}^*$, where $\mu_J$ and $\mu_A$ are defined in (2) (see (15)). Also, there exists $k_0 \in \mathbb{N}$ such that for each $k \geq k_0$ there exists a hyperbolic equilibrium point $\overrightarrow{N}_k^* \in \mathbb{R}^{2N}$ of system (1) such that*

$$\lim_{k\to\infty}\overrightarrow{N}_k^* = \overrightarrow{N}^*$$

1. *If $\overrightarrow{n}^*$ is asymptotically stable then $\overrightarrow{N}_k^*$ is asymptotically stable for each $k \geq k_0$, and the basins of attraction of each $\overrightarrow{N}_k^*$ can be described in*

*terms of the basins of attraction of* $\vec{n}^*$.

2. *If* $\vec{n}^*$ *is unstable then* $\overrightarrow{N_k}^*$ *is unstable, for each* $k \geq k_0$.

*The previous results hold for hyperbolic periodic solutions of the aggregated system.*

**Proof.** See comments at the end of Appendix A.1. □

## 3. Analysis of the model

We are obviously interested in ascertain whether the population goes extinct or not and, if not, its long term behavior. A first observation is that $\vec{n} = \vec{0}$ is a solution of system (4); whether $\vec{n} = \vec{0}$ is stable or unstable determines whether the population goes extinct or not.

Both the complete system (1) and the aggregated system (4) are well defined, meaning that both systems evolve within the corresponding non-negative cones, since all of the coefficients involved in the equations are non negative. The following result states that the solutions of the aggregated system are bounded regardless of the (non negative) initial values; a similar result can be derived for the complete system (it cannot be derived from Theorem 2.1, but the proof is similar).

**Theorem 3.1.** *There exists* $0 < M \in \mathbb{R}$ *such that for any* $\vec{n} \in \overline{\mathbb{R}}^2_+$ *with* $\|\vec{n}\| \geq M$ *it holds that*

$$\|\mathscr{L}(\vec{n})\| \leq \|\vec{n}\|$$

**Proof.** From the definition of map $\bar{s}$ in (4) we get that

$$\|\bar{s}(\vec{n})\| \leq |\overline{\sigma}_J|J| + |\overline{\sigma}_A|A| + |\overline{\phi}(J, A)||A|. \tag{6}$$

Besides, using (5), it follows that

$$\overline{\sigma}_J \leq \sigma_J := \max\{\sigma_J^1,\ \sigma_J^2\} < 1, \qquad \overline{\sigma}_A \leq \sigma_A := \max\{\sigma_A^1,\ \sigma_A^2\} < 1.$$

Therefore, using the previous bounds in (6) we get that

$$\|\bar{s}(\vec{n})\| \leq (\max\{\sigma_J,\ \sigma_A\} + |\overline{\phi}(\vec{n})|)\|\vec{n}\|.$$

We have assumed that $\lim_{\|x\|\to\infty}\phi_i(\vec{x}) = 0$, for $i = 1, \ldots, N$. Then, there exists $M > 0$ such that $\phi_i(\vec{x}) < 1 - \max\{\sigma_J,\ \sigma_A\}$ for any $\vec{x}$ such that $\|\vec{x}\| \geq M$, which finishes the proof. □

### 3.1. Population survival and dispersal

The survival of the population can be analyzed by means of the stability of the zero solution. Remarkably, the reduced system is driven by a density-dependent Leslie matrix. In this context, a key quantity characterizing the long term behavior of the system is the *inherent net reproductive number* denoted here by $\nu$ which, according to [11], is "the expected number of offspring (for each newborn) over the course of its entire lifetime". From a mathematical point of view, $\nu$ is the spectral radius of the so-called next generation matrix and, biologically [9] represents the distribution with respect to state-at-birth of all newborn descendants accumulated during the entire lifespan of an age structured population $\overrightarrow{N_0}$. If $\nu > 1$ the population will survive while if $\nu$ is less than 1 the population may go extinct.

For the shake of completeness we have sketched in Appendix A.2 (see also [9,11]) the calculations leading to the *(global) inherent net reproductive number*

$$\overline{\nu} := \overline{\phi}(\vec{0})\frac{\overline{\sigma}_J}{1 - \overline{\sigma}_A} \tag{7}$$

that extends the (local) inherent net reproductive number

$$\nu_i = \phi_i(0)\frac{\sigma_J^i}{1 - \sigma_A^i} \tag{8}$$

at patch $i = 1, \ldots, N$ by combining the local fertility and survival rates weighted by the asymptotic distribution of individuals of each age class.

The parameter $\overline{\nu}$ is not explicit in system (4) but it is easy to make it appear (see Appendix A.2). The following result, a rephrasing [11, Theorem 1.7] characterizes the stability of the zero solution

**Theorem 3.2.** *Consider system (4) and its inherent net reproductive number* $\nu$ *given by (7). Then,*

1. *The zero solution* $\vec{0}$ *is locally asymptotically stable if* $\overline{\nu} < 1$.
2. *The zero solution* $\vec{0}$ *is unstable if* $\overline{\nu} > 1$.

**Proof.** It is straightforward to check that system (4) fulfills the hypotheses that lead to [11, Theorem 1.7]. □

It is of interest to understand whether the fact of connecting patches changes the dynamics of the (local) populations. We will use either "local" or "global" whenever we refer to unconnected or connected patches, respectively.

**Theorem 3.3.** *Consider system (4). Then,*

1. *The zero solution* $\vec{0} \in \mathbb{R}^2$ *is globally asymptotically stable if*

$$\frac{\max_i\{\phi_i(\vec{n}),\ \vec{n} \in \mathbb{R}^2\}\max_i\{\sigma_i^J\}}{1 - \max_i\{\sigma_i^A\}} < 1 \tag{9}$$

2. *The zero solution* $\vec{0} \in \mathbb{R}^2$ *is unstable if*

$$\frac{\min_i\{\phi_i(\vec{0})\}\min_i\{\sigma_i^J\}}{1 - \min_i\{\sigma_i^A\}} > 1 \tag{10}$$

**Proof.** First, note that

$$\begin{pmatrix} 0 & \overline{\phi}(\vec{n}) \\ \min_i\{\sigma_i^J\} & \min_i\{\sigma_i^A\} \end{pmatrix} \leq \begin{pmatrix} 0 & \overline{\phi}(\vec{n}) \\ \overline{\sigma}_J & \overline{\sigma}_A \end{pmatrix} \leq \begin{pmatrix} 0 & \max_i\{\phi_i\} \\ \max_i\{\sigma_i^J\} & \max_i\{\sigma_i^A\} \end{pmatrix}$$

where the inequalities are entry-wise. Regarding 1, any solution of system (4) is bounded from above by the solution of the discrete system driven by most right hand side transition matrix in the above inequality. From [19, Theorem 5.612], condition (9) leads the bounding solution to $(\vec{0})$. On the other hand, 2 follows from [11, Theorem 1.7]. □

Thus, roughly speaking, if $\phi_i \approx \phi_j$, $\sigma_i^J \approx \sigma_j^J$ and $\sigma_i^A \approx \sigma_j^A$ for all $i \neq j$, $i, j = 1, \ldots, N$, the differences between the local and the global behavior are expected to be tiny. However, connecting heterogeneous patches may lead to surprising outcomes.

#### 3.1.1. Linking source–source, sink–sink or source–sink patches

We distinguish two kind of patches: sources and sinks. A source is that patch where a population is viable (the zero solution is unstable) and a sink patch is the contrary (and the zero solution is globally asymptotically stable). It is accepted that dispersal cannot affect the survival (resp. extinction) of a metapopulation consisting of source-source (resp. sink-sink) patches [15,18]. The aforementioned results do not account for age structure and our results are consistent with this claim when either condition (9) or (10) hold, but we have also found that it is not necessarily true when these conditions fail. This (apparently) counterintuitive result is directly related to the age structure of the population and the fact that age classes distribution can be heterogeneous. To our knowledge, the following results are completely new. We consider just a two patches environment since this settings are sufficient to show our results.

*Source–source.* The next result displays sufficient conditions under which connecting two viable populations leads to extinction the local populations, i.e, to connect two source patches leads the resulting

metapopulation to extinction. This result can be easily generalized to $N$ patches.

The idea is as follows: assume that in one patch adult survival is low but compensated by a high juvenile survival and, conversely, in the other patch juvenile survival is low but compensated by a high adult survival. The tradeoff mechanism can be broken by an inappropriate age classes dispersal and a plausible scenario is the following: in fish populations consider close to versus away from a reef in the presence of a predator. When away from the reef, weaker individuals (juveniles) are more vulnerable to predators (lower survival rate) while close to the reef region, smaller individuals find more places where to hide (refuges) so that juvenile are more likely to survive than adults. As a consequence, the distribution of age classes is likely to be heterogeneous. The conditions on the parameters of the model in the following theorem should be understood as one (of many) ways to concrete these ideas.

**Theorem 3.4.** *Consider system (4) such that* $\phi_i(\vec{0}) > 1$. *Let us assume that*

$$\sigma_1^J = 1 - \sigma_1^A, \qquad \sigma_2^A = 1 - \sigma_1^A, \qquad \sigma_2^J = 1 - \sigma_1^J, \qquad \mu_1^J = 1 - \mu_1^A \tag{11}$$

*with* $\sigma_i^\theta, \mu_i^\theta \approx / \ 1/2$ *(note that* $\nu_i > 1$ *for* $i = 1, 2$*). Then,* $\overline{\nu} < 1$ *if, and only if,*

$$\frac{\overline{\phi}(\vec{0})}{1 + \overline{\phi}(\vec{0})} < \mu_A(1 - \sigma_1^A) + \sigma_1^A(1 - \mu_A). \tag{12}$$

**Proof.** Condition (12) follows by direct calculations from the definition of $\overline{\nu}$ in (7) and the asymmetry conditions (11). □

Note that because of the continuity of $\overline{\nu}$ respect to the parameters defining it, Theorem 3.4 holds for small perturbations in conditions (11) (i.e., by replacing the equals sign "=" by "approximately the same" ( ≈ )).

Theorem 3.4 says that the local populations would survive if unconnected (since $\nu_i > 1$) but the resulting connected metapopulation would globally collapse because of the heterogeneous age classes spatial distribution. Note that otherwise, i.e., if $\mu_i^J$ is sufficiently similar to $\mu_i^A$, the population would globally survive. Fig. 2 displays the inherent net reproductive numbers: the local ones (see (8), discontinuous gray lines for isolated patches, note that $\nu_i > 1$) and the global one (solid black line, $\overline{\nu}$, see (7)) as function of the dispersal parameter $\mu_1^J$. On the left panel, the age classes structure is homogeneous ($\mu_i^A = \mu_i^J$). On the right panel, the age classes structure is allowed to be unbalanced : $\overline{\nu} > 1$ for $\nu_1^J \approx 0$ while $\overline{\nu} < 1$ for $\nu_1^J \approx 1$, where $\mu_1^A = 1 - \mu_1^J$.

*Sink–sink.* In a symmetric manner to the source-source case described in above, the model allows parameter values such that a metapopulation consisting of two sink patches can survive in the long term, even though the isolated population would disappear at each patch if isolated. For the sake of brevity, we omit the equivalent of Theorem 2 that can be easily written by the interest reader. We include instead a numerical simulation in Fig. 3.

*Source–sink.* It is known that when the spatial model consists of source-sink patches, there exist specific dispersal rates may lead to either global population survival or global collapse [15] (and references therein). Our results are consistent with those although, in addition, we have found that the shape of the age-structure density-dependent fertility functions together with dispersal may lead to either linear or non-linear transitions between dispersal-induced survival/collapse outcomes. See Section 4 for further comments.

### 3.2. Stability of the positive equilibrium states

Up to now we have characterized the stability of the zero solution $\vec{0}$ by means of the values of the inherent net reproductive number $\overline{\nu}$. The set of pairs $\{(\overline{\nu}, \vec{0});\ \overline{\nu} \in \mathbb{R}\}$ is a curve of the extinction solutions of system (4) in $\mathbb{R}^3$, the so-called trivial branch. From a dynamical point of view such a extinction solution is locally stable for $\overline{\nu} < 1$ and unstable for $\overline{\nu} > 1$. In the later case, if the population does not go extinct, where does it go? We already know that population remains bounded, and the question is whether there are other (positive) equlibrium points that attract the solution of system (4) as $\overline{\nu}$ crosses the threshold value $\overline{\nu} = 1$. Furthermore, is extinction the only possible outcome for $\overline{\nu} \sim 1$, $\overline{\nu} < 1$, or is there strong Allee effects?

We face this question by seeking for the existence of another curve $\{(\overline{\nu}, \vec{n}^*);\ \overline{\nu} \sim 1\}$ of no negative solutions of system (4) that meets (*bifurcates*) the trivial branch at $(1, \vec{0})$. We apply bifurcation techniques to the aggregated system (4) to answer this questions and Theorem (2.1) to translate this analysis to the complete system (1). The net inherent reproductive number is usually used as bifurcation parameter. Let us introduce few simple concepts on bifurcation.

We denote $\Sigma \subset \mathbb{R}^3_+$ the set of pairs $(\overline{\nu}, \vec{n}^*)$ where $\vec{n}^*$ is an equilibrium point to system (4). We call *continuum* any closed connected set. We denote

$$\mathscr{C}_0 = \{(\overline{\nu}, \vec{0});\ \nu \in \mathbb{R}\} \subset \Sigma$$

the above mentioned trivial branch. The following result establishes conditions for the existence of a continuum bifurcating from $\mathscr{C}_0$ at $\overline{\nu} = 1$

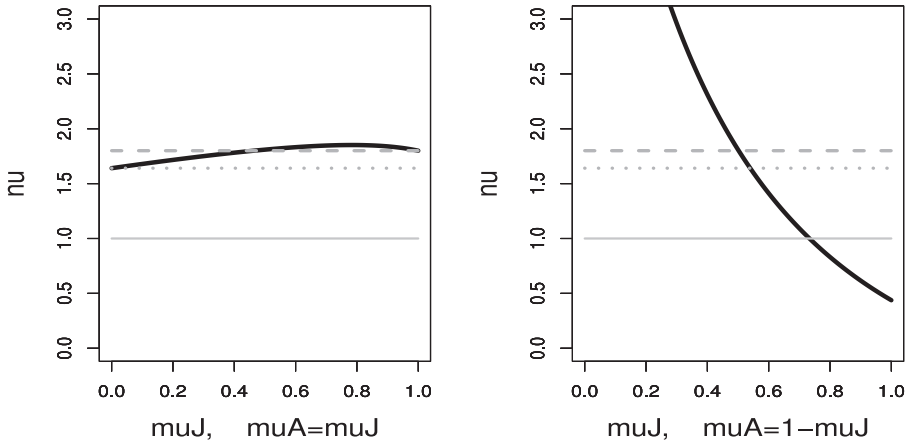


**Fig. 2.** Inherent net reproductive numbers as function of $\mu_J \in [0, 1]$, the local ones in gray (see expression (8), dashed line for patch 1 and dotted line for patch 2, $\nu_i > 1$) and the global one (see expression (7)) in solid black line. On the left, the age classes dispersal is homogeneous ($\mu_1^A = \mu_1^J$) and $\nu$ remains above the threshold value 1. On the right, the age classes dispersal is heterogeneous: $\overline{\nu} > 1$ for $\nu_1^J \approx 0$ while $\overline{\nu} < 1$ for $\nu_1^J \approx 1$, where $\mu_1^A = 1 - \mu_1^J$. Parameter values: $\sigma_1^J = .2$, $\sigma_1^A = .75$, $\phi_1(\vec{0}) = 2.25$, $\sigma_2^J = .75$, $\sigma_2^A = .2$ and $\phi_2(\vec{0}) = 1.75$.

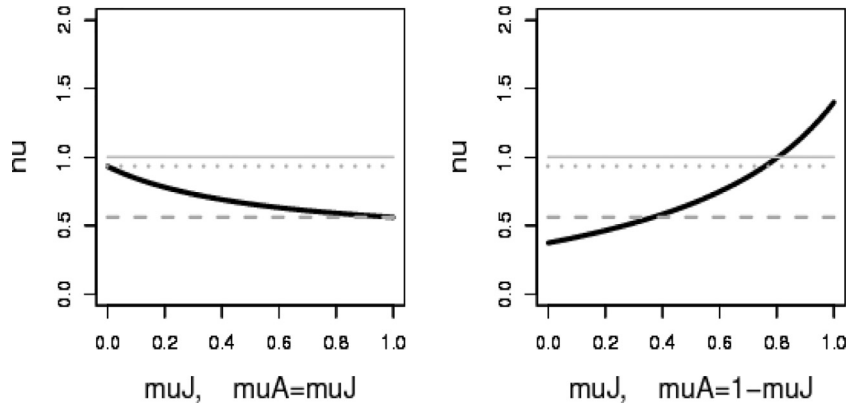


**Fig. 3.** Local inherent net reproductive numbers (see expression (8), in gray, dashed line for patch 1 and dotted line for patch 2, $\nu_i < 1$) and the global inherent net reproductive number $\overline{\nu}$ (see expression (7), solid black line) as function of $\mu_J \in [0, 1]$. On the left panel age classes dispersal is homogeneous ($\mu_A = \mu_J$) and $\overline{\nu}$ remains below the threshold value 1. On the right panel age classes dispersal is heterogeneous: $\overline{\nu} < 1$ for $\nu_1^J \approx 0$ while $\overline{\nu} > 1$ for $\nu_1^J \approx 1$, $\mu_1^A = 1 - \mu_1^J$. Parameter values: $\sigma_1^J = .5$, $\sigma_1^A = .2$, $\phi_1(\vec{0}) = 1.3$, $\sigma_2^J = .2$, $\sigma_2^A = .7$ and $\phi_2(\vec{0}) = 1.4$.

to positive equilibrium, that is, a pair $(\overline{\nu}, \vec{n}^*)$ with $\vec{n}^* > (\vec{0})$ and $\overline{\nu} \sim 1$.

**Theorem 3.5.** *Consider system (4) and assume that the fertility functions are such that $\phi_i \in C^1(\overline{\mathbb{R}}^2_+, \mathbb{R}_+)$. Then, there exists a continuum $\mathscr{C}_+$ in $\overline{\Sigma}$ such that*

- $(1, \vec{0}) \in \mathscr{C}_+$.
- $(\overline{\nu}, \vec{n}) \in \mathscr{C}_+ \setminus (1, \vec{0})$ *and* $\overline{\nu} > 1$, *and the components of* $\vec{n}$ *are positive.*
- $\mathscr{C}_+ \setminus (1, \vec{0})$ *is unbounded in* $(1, \infty) \times \mathbb{R}^2_+$.

**Proof.** See Appendix A.2. □

Once established the existence of positive equilibrium states, the focus is on their stability, since the bifurcation from the trivial branch $\mathscr{C}_0$ can be to either stable or unstable positive equilibrium points (the later case is related to the Allee effect [11]). Which alternative occurs depends on the sign of the *(global) direction of bifurcation* $\overline{\kappa}$, *[11]* defined by

$$\overline{\kappa} = -\overline{\sigma}_J \left( \overline{\phi}(\vec{0}) \frac{\partial \overline{\phi}(\vec{0})}{\partial J} + \frac{\partial \overline{\phi}(\vec{0})}{\partial A} \right), \tag{13}$$

derived in Appendix A.2. Note that the sign of $\overline{\kappa}$ depends on the derivatives with respect to $J$ and $A$ of the (local) fertility functions. Both the global inherent net reproductive number and the global direction of bifurcation are built upon the local parameters of the model but determine its global behavior. Their meaning is the same as the inherent net reproductive number and the direction of bifurcation, but are meaningful at different scales (global versus local).

We first assume that both fertility functions belong to the same class C1 or C2 at both patches. In short, our result say that the global behavior reproduces the local behavior if patches were isolated.

On the one hand, for those populations with C1 fertility function, there are no component Allee effects and the bifurcation in Theorem 3.5 is *supercritical*. That means that the positive equilibrium states are locally asymptotically stable and the zero equilibrium is unstable, at least in a neighborhood $(1, 1 + \delta)$ of the bifurcation threshold $\nu = 1$ value, for certain $\delta > 0$.

**Theorem 3.6.** *Consider system (4) and assume that fertility functions $\phi_i \in C^1(\overline{\mathbb{R}}^2_+, \mathbb{R}_+)$ belong to class C1 for $i = 1, ..., N$. Then, the bifurcation branch $\mathscr{C}_+$ in Theorem 3.5 is supercritical.*

**Proof.** It follows from [11, Theorem 2.3] by explicitly calculating the bifurcation direction $\overline{\kappa}$ (see Appendix A.2). Direct calculations lead to $\overline{\kappa} > 0$ since $\phi_i$ is strictly decreasing in both $J$ and $A$, which means that It follows from [11, Theorem 2.3] by explicitly calculating the bifurcation direction $\overline{\kappa}$ (see Appendix A.2). Direct calculations lead to $\overline{\kappa} > 0$ since $\phi_i$ is strictly decreasing in both $J$ and $A$, which means that the bifurcation is supercritical. □

On the other hand, for those populations with C2 fertility function there are component Allee effects and the bifurcation in Theorem 3.5 is *subcritical* (see the discussion Section 4). That means that the positive equilibrium states are locally asymptotically unstable at least in a neighborhood $(1 - \delta, 1)$ of the bifurcation threshold $\overline{\nu} = 1$ value, for certain $\delta > 0$.

**Theorem 3.7.** *Consider system (4) and assume that the fertility functions $\phi_i \in C^1(\overline{\mathbb{R}}^2_+, \mathbb{R}_+)$ belong to class C2 for $i = 1, ..., N$. Then, the bifurcation branch $\mathscr{C}_+$ in Theorem 3.5 is subcritical.*

**Proof.** See the proof of Theorems 3.6. In this case, the hypothesis imply that the bifurcation direction $\overline{\kappa}$ given by (13) is negative, which implies that the bifurcation is subcritical. □

Fig. 4 displays simulations in two patches environment that illustrate the above results: the typical supercritical (left, both fertility functions belong to class C1) and subcritical (right, both fertility functions belong to class C2) bifurcation diagrams. Note that in the right panel, for $\overline{\nu} \approx (0.2, 2)$ there exists other equilibrium attractor than the zero solution; and what is the outcome of the model depends on the initial values, what is called *strong Allee effect,Cushing14*. Further details on the precise expression of the functions involved in the construction of the bifurcation diagram, the values of the parameters and suitable code (written in R) to reproduce the diagrams can be found in the *reproducible code document* [16].

The following result deals with all the other situations, i.e., when either both fertility functions belong to class C3 or each fertility function belongs to a different class (C1, C2, C3). That is, there are component Allee effects only in some patches. It is shown that in such a case there exist always dispersal schemes yielding either $\overline{\kappa} < 0$ or $\overline{\kappa} > 0$, what means the weight of the component Allee effects at the metapopulation level depend on the asymptotic distribution of individuals among patches.

**Theorem 3.8.** *Consider system (4) and assume either*

- *That both fertility functions $\phi_i$ belong to class C3.*
- *Or that each fertility function belongs to a different class (C1, C2, and C3).*

*Then, there are dispersal schemes leading to either a subcritical or a supercritical bifurcation to positive solutions.*

**Proof.** See Appendix A.2. □

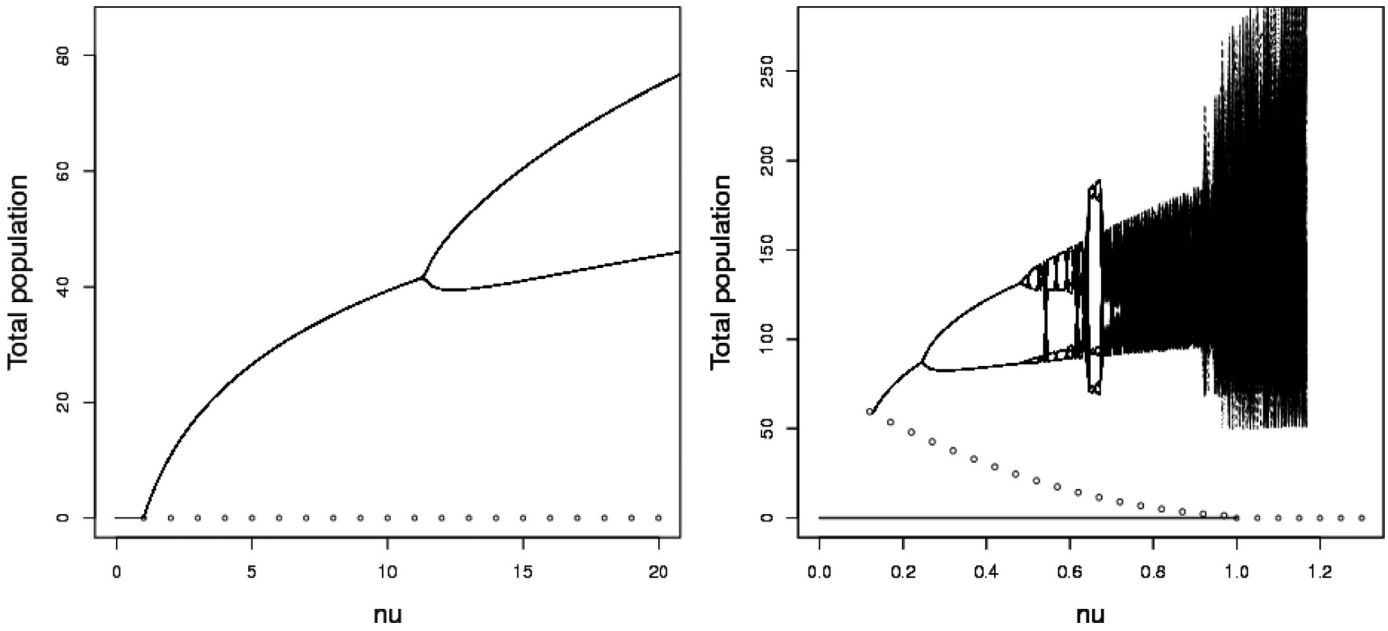


**Fig. 4.** Bifurcation diagram, total population size versus $\bar{\nu}$. Local fertility functions of class C1 (left, supercritical, $\phi_i(J_i, A_i) = \psi_i \cdot \exp(-a_J^i J_i - a_A^i A_i))$, $i = 1, 2$) and C2 (right, subcritical, $\phi_i(J_i, A_i) = \psi_i \cdot (1 + J_i A_i)\exp(-a_J^i J_i - a_A^i A_i))$, $i = 1, 2$). Besides, for both functions, $a_J^1 = a_A^1 = 0.1$, $a_J^2 = a_A^2 = 0.2$, $\sigma_{J_1} = 0.2$, $\sigma_{J_2} = 0.75$, $\sigma_{A_1} = 0.85$, $\sigma_{A_2} = 0.3$, $p_1^J = 0.4$, $p_2^J = 0.4$, $p_1^A = 0.4$, $p_2^A = 0.4$, $\psi_1$ ranges from 0 to 30 by an steep equal to 0.1 and $\psi_2$ ranges from 0 to 15 by an steep equal to 0.05. For the construction of the bifurcation diagrams, for each value of the bifurcation parameter $\bar{\nu}$ we have set up initial values, run 1000 iterates of the aggregated model, discarded the first 800 and plot the last 200. This procedure captures just attractor sets. In the right panel, the bifurcation at $\bar{\nu} = 1$ is to unstable equilibrium points (not solid points). At a given point there is a blue sky type bifurcation and the backwards unstable branch turns to the right and becomes stable. We have not calculated the branch of unstable equilibrium points, since its precise shape is not relevant to our problem and we have just plotted a polynomial curve joining both the trivial branch $\mathscr{C}_0$ and the nontrivial branch of stable equilibrium points. In both panels, there are a subsequent period doubling bifurcation(s). Full information and code is available in the reproducible document [16].

## 4. Conclusions

This work was aimed to analyze the interplay between dispersal strategies and density-dependent fertility in a metapopulation structured by age. We have included the age structure in both dispersal and fertility processes under the assumption that individuals dispersal and demography are processes that evolve according to different time scales.

### 4.1. Connecting sources and/or sinks

From the environmental management perspective, it is fundamental not only considering the properties of the patch to patch connections and those of the connected patches [2], but also the dispersal tendencies of individuals of different age classes [1]. Our results complement those found in [15,18].

*A comment on source and sink patches*. Regarding sink regions, some authors [3] suggest that an inaccurate evaluation of the habitat quality may lead species to settle on a sink region and, indeed it was shown later [33] that it is not always easy to decide whether a given habitat is a good one to settle. Our results reinforce these assertions, since we have seen that connecting two source (sink) patches may lead the resulting metapopulation to extinction (survive).

*Disperal-induced global source-sink behavior*. When the spatial model consists of source–sink patches, there exist dispersal schemes that may lead to either global population survival or global collapse [15] (and references therein). Indeed, there exists a threshold for dispersal rates leading the source-sink system to either survive or go extinct. Once this threshold is established, from a management point of view, it is of interest to know the sensitivity of the outcome to variations on the dispersal rates.

From expression (7) defining $\bar{\nu}$ it can be seen that when survival rates are spatially homogeneous (i.e., $\sigma_i^J \approx \sigma_j^J$ and $\sigma_i^A \approx \sigma_j^A$ for all $i \neq j$) the transition from behaving as a global sink to a global source as the asymptotic distribution of individuals changes from the local sink to the local source is (almost) linear. Otherwise, in the heterogeneous case, nonlinear transitions can be observed. Thus, slight variations in dispersal rates may lead to abrupt variations in the global inherent net reproduction number, making the global population either survive or collapse. We illustrate these facts in Fig. 5 in a two patches environment.

### 4.2. On the Allee effect: local density-dependent fertility functions and dispersal

The Allee effect is recognized to have great importance in ecology [10,12] and many efforts have been dedicated to analyze the interplay between the Allee effect and dispersal (see [14] and references therein). A negative sign in the direction of bifurcation $\bar{\kappa}$ [11,12] entails for Allee effect and, in our framework, it has to do with the existence of strong enough component Allee effects in local fertility functions.

From a management point of view, the intervention strategies aimed to avoid the Allee effect spin around the idea of keeping the population away from the Allee threshold, what can be done by connecting this patch to a source patch that supplies individuals.

Theorem 3.6 tell us that whenever $\phi_i$ are of class C1, $i = 1, ...,N$, there are no component Allee effects while, if $\phi_i$ are of class C2, $i = 1, ...,N$, from Theorem 3.7 the possibility of an Allee effect episode is intrinsic to the population. In Theorem 3.8 we found that when the fertility functions are of different type at each patch (or all of them of type C3) the sign of $\bar{\kappa}$ can be either positive or negative and it depends on the dispersal rates, that define the strength of the component Allee effects at the metapopulation level. Thus, there is room to avoid further

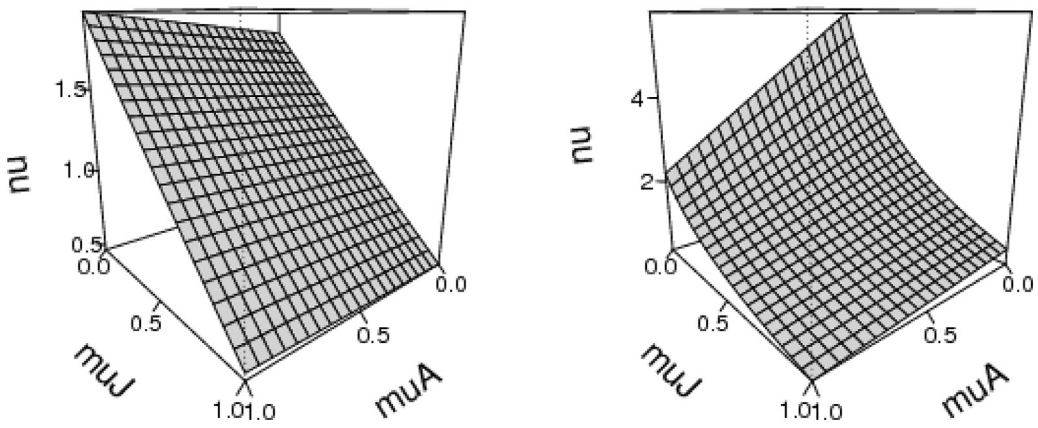


**Fig. 5.** Global inherent net reproductive number (see (7)) as function of juvenile and adult asymptotic spatial distribution in a two patches environment. Left panel $\sigma_1^J = 0.52$, $\sigma_2^J = 0.48$, $\sigma_1^A = 0.38$, $\sigma_2^A = 0.41$, $\phi_1(\vec{0}) = 0.6$, $\phi_2(\vec{0}) = 2.2$. Right panel $\sigma_1^J = 0.3$, $\sigma_2^J = 0.8$, $\sigma_1^A = 0.2$, $\sigma_2^A = 0.7$, $\phi_1(\vec{0}) = 0.6$, $\phi_2(\vec{0}) = 2.2$.

Allee effects as far as managers keep control on dispersal.

Interestingly, the existence of a patch without component Allee effects (in the fertility function) is a necessary but not a sufficient condition (actuation): it is just the basis that makes it possible to avoid Allee episodes via the control of local vital rates (see comments below on Fig. 6). These last comments apply also to the implementation of terrestrial refuges [31], marine protected areas or artificial habitats (e.g. reefs) that are also broadly used for population management purposes, in order to create source patches that help to maintain endangered populations as well as to enhance exploited populations [6,40] (obviously, those are not a universal solution [23]).

The previous statements are general ones and do not depend on the age structure of the population. Nevertheless, as illustrated in Fig. 6, when the population is age structured the sign of $\overline{\kappa}$ is sensitive to homogeneous/heterogeneous age classes distribution (in a two patches environment). In Fig. 6 we assume that $\phi_1$ is of class C1 and $\phi_2$ of class C2 and we represent the bifurcation direction $\overline{\kappa}$ as function of dispersal rates and and intrinsic local fertility rates. In the left panel of Fig. 6 we suppose that juvenile and adult individuals are homogeneously mixed ($\mu_1^J = \mu_1^A$) while in the right panel juvenile and adult individuals mainly disperse asymmetrically ($\mu_1^A = 1 - \mu_1^J$, $\mu_1^A \approx / \ \mu_1^J$) For the chosen parameter values and for any fixed value of $\alpha$ (the difference between local intrinsic fertility rates) there are values of the dispersal rates yielding bifurcation to either unstable ($\overline{\kappa} < 0$) or stable ($\overline{\kappa} > 0$) equilibrium states.

### 4.3. Further effects on the population size and (de)stabilization phenomena

A recent work [15] deals with the effects on the population fitness of connecting two patches. The authors considered symmetrical dispersal (meaning that the fraction if individuals leaving each patch is the same) in a population without age classes structure and found that connecting source-source patches may increase the global population size; furthermore, in particular, the curve displaying population size versus dispersal rate was unimodal.

Our results are complementary to those in [15]. On the one hand, when age classes dispersal is homogeneous all the numerical experiments performed show that the aforementioned curve is unimodal. We could not provide an analytical (mathematical) proof since the equations become too complicated due to consider age structure. On the other hand, the curve is not necessarily unimodal when age classes distribution is heterogeneous (right panel in Fig. 7).

Fig. 7 consists of two bifurcation diagram displaying the total population size versus the asymptotic distribution of individuals between two connected patches (black solid line) along with its distribution among patch 1 (black dotted line) and patch 2 (black dashed line). On the left panel $\mu_A = \mu_J$ (homogeneous dispersion) and on the right panel $\mu_A = 1 - \mu_J$, (focus on the region where i.e heterogeneous age classes dispersal). The lines in gray represent the population size at patch 1 (dashed), at patch 2 (dotted) and the total population size (dotted–dashed) when patches are isolated. Note that on the left panel the total population size equals the local population size at patch 2 at $\mu_J = \mu_A = 0$ (all the individuals are in patch 2) and equals the local population size at patch 1 at $\mu_J = \mu_A = 1$ (all the individuals are in patch 1).

Away from the bifurcation to positive equilibrium points at $\overline{\nu} = 1$, further bifurcations are possible, as doubling period and routes to chaos. Many previous works have addressed the effects of dispersal on

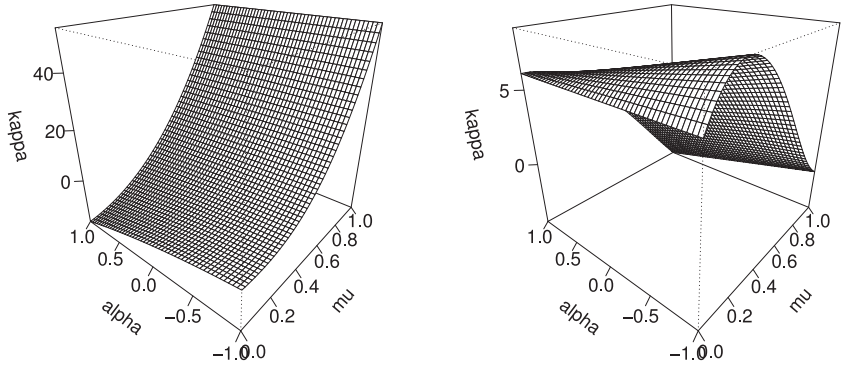


**Fig. 6.** The bifurcation direction $\overline{\kappa}$ (see (13)) depends on dispersal rates and intrinsic fertility rates. Local fertility functions are of class C1 and C2 (further details can be found in the reproducible code document [16]). Parameter values $\phi_1(\vec{0}) = 2$, $\phi_2(\vec{0}) = \phi_1(\vec{0}) + \alpha$, $\alpha \in [-1, 1]$, $\sigma_1^J = 0.75\sigma_2^J = 0.75$. On the left panel, dispersal is homogeneous between age classes for $\mu_1^J \in [0, 1]$, $\mu_1^A = \mu_1^J$. On the right, age classes distribution is allowed to be heterogeneous $\mu_1^J \in [0, 1]$, $\mu_1^A = 1 - \mu_1^J$, $\mu_1^A \not\approx \mu_1^J$.

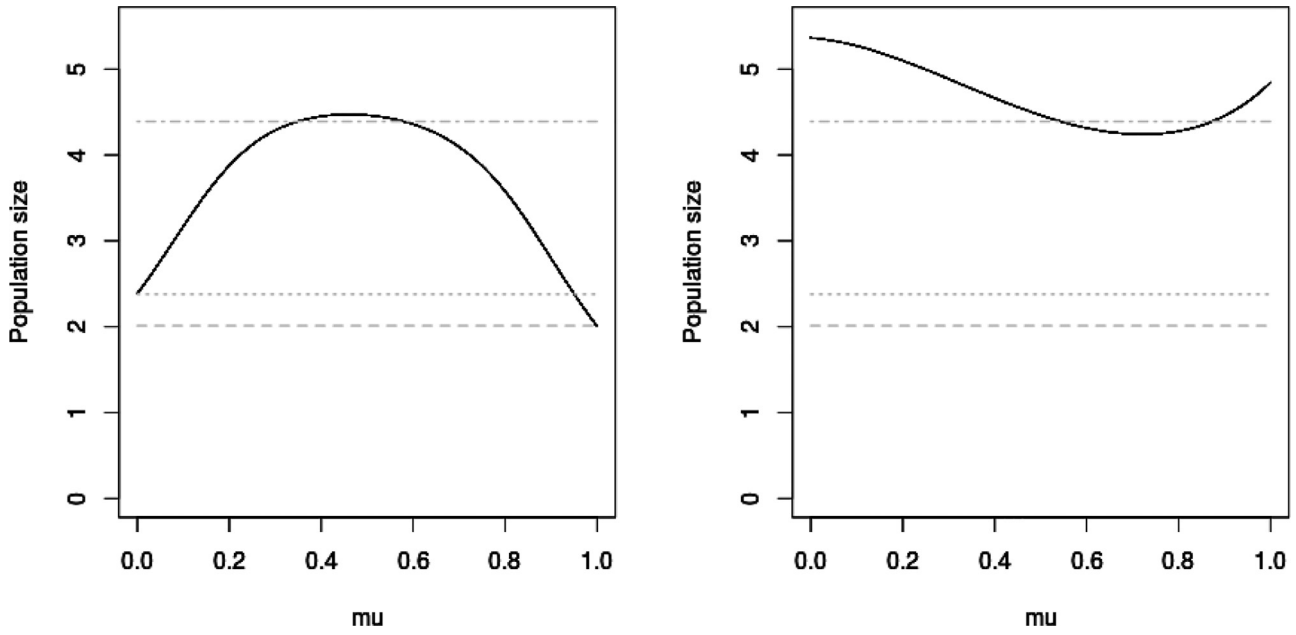


**Fig. 7.** The black line represents a bifurcation diagram displaying the total population size versus the asymptotic spatial distribution of individuals between two connected patches: on the left $\mu_A = \mu_J$ (homogeneous dispersal) and on the right $\mu_A = 1 - \mu_J$, $\mu_A \approx \mu_J$ (heterogeneous dispersal). The lines in gray represent the population size at patch 1 (dashed), at patch 2 (dotted) and the total population size (dotted-dashed) when patches are isolated. Fertility functions belong to class C1, namely, $\phi_i(J_i, A_i) = \psi_i \exp(-a_J^i J_i - a_A^i A_i)$ with $a_J^1 = a_A^1 = 0.1$, $a_J^2 = a_A^2 = 0.2$ and $\psi_1$ ranging from 0 to 30 by an steep equal to 0.1 and $\psi_2$ ranging from 0 to 15 by an steep equal to 0.05. Besides, $\sigma_1^J = 0.4$, $\sigma_2^J = 0.6$, $\sigma_1^A = 0.4$, $\sigma_2^A = 0.3$, $\phi_1(\vec{0}) = 5$ and $\phi_2(\vec{0}) = 5.5$. The diagram is built as in Fig. 4. The code to compute the diagram can be found in [16].

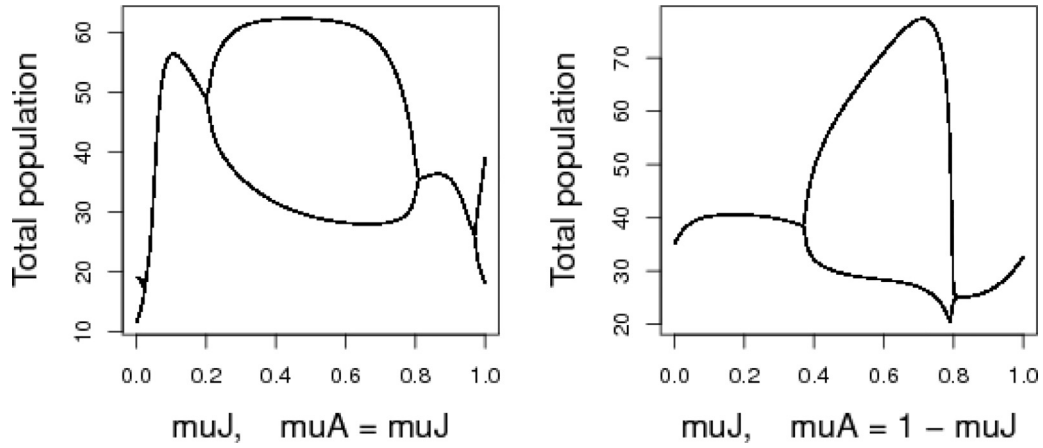


**Fig. 8.** The black line represents a bifurcation diagram displaying the total population size versus the asymptotic distribution of individuals between connected patches: on the left $\mu_A = \mu_J$ and on the right $\mu_A = 1 - \mu_J$ $\mu_A \approx \mu_J$ (heterogeneous age classes distribution). Fertility functions belong to class C1, namely $\phi_i(J_i, A_i) = \psi_i \exp(-a_J^i J_i - a_A^i A_i)$ with $a_J^1 = a_A^1 = 0.1$, $a_J^2 = a_A^2 = 0.2$ and $\psi_1$ ranging from 0 to 30 by an steep equal to 0.1 and $\psi_2$ ranging from 0 to 15 by an steep equal to 0.05. The other parameter values are $\sigma_{J_1} = 0.2$, $\sigma_{J_2} = 0.6$, $\sigma_{A_1} = 0.85$, $\sigma_{A_2} = 0.3$ The code to compute the diagram can be found in [16].

stabilization/destabilization of a population model (see [13] and references therein). Including age structure in the populations model and considering homogeneous/heterogeneous age classes distribution should lead to a wider range of outcomes. An exhaustive study of possible outcomes is beyond the scope of this work and we think that it deserves attention in future works. For instance, the following Fig. 8 displays the local population size at each patch when patches are isolated, that are attracted by a 2-cycle, respectively (see the leftmost/rightmost hand sides of the curve in the left panel). When patches are connected and age classes distribution is homogeneous (left panel), the global population dynamics displays still a 2-periodic behavior when $\mu_A = \mu_J \in [0, \delta) \cup (0.2, 0.8) \cup (1 - \delta, 1]$ (approx). Nevertheless, there are two ranges of asymptotic individuals distribution that globally stabilize the total population size when $\mu_A = \mu_J \in (0.2, 0.8)$ (approx).

On the contrary, when age classes distribution is allowed to be heterogeneous (right panel), the global population dynamics does *not* display a 2-periodic behavior for strong enough asymmetrical distribution ($\mu_A = 1 - \mu_J$ and $\mu_J \in [0, 0.38] \cup [0.78, 1]$, approx) but the global behavior is 2-periodic when $\mu_J \in (0.38, 0.78)$ (approx). Let us recall that it follows from Theorem 2.1 that global periodic behavior implies local periodic behavior.

Up to date, approximate aggregation techniques do not allow to translate information about general compact attractors different from hyperbolic equilibrium points or periodic solutions from the aggregated system to the general one. Preliminary numerical simulations have revealed a wide range of behaviors challenging our intuition, and we hope that his findings encourage further development of approximate aggregation techniques allowing to complete such an analysis.

#### 4.3.1. *Highlights*

We conclude by highlighting the key ideas and conclusions

- Our results are coherent with those in the existing literature when there is spatial homogeneity and homogeneous age classes dispersal, although otherwise the model allows unexpected outcomes.
- The long term behavior of the population is sensitive to both the dispersal rates of individuals belonging to different age classes and the shape of the fertility function.
- Managers may expect to keep some control on the population dynamics through the global direction of bifurcation $\overline{\kappa}$ and the global inherent net reproductive number $\overline{\nu}$ insofar as they (managers) can modify dispersal or local vital rates.
- At the landscape scale, alterations that modify species dispersal strategies may drastically change the long term behavior of the whole metapopulation.
- At the local (patch) scale, alterations of the habitat may have repercussion at the global scale via individuals dispersal.
- Implementing refuges or artificial habitats may not be enough to preclude Allee effect episodes in the metapopulation, meaning that even the subpopulation inhabiting the refuge would be exposed to the Allee efect given appropriate dispersal rates.

**Acknowledgment**

M. Marvá and F. San Segundo are supported by Ministerio de Ciencia e Innovación (Spain), project MTM2014-56022-C2-1-P. The authors thanks R. Bravo de la Parra for the hint on the proof of Theorem 3.8.

## Appendix A

### A1. Reduction dimension procedure

In this section, we describe in a more detailed way the approximate aggregation procedure applied to system (1) in order to derive the aggregated system (4). The starting point is the two time scales system (1)

$$X_{n+1} = \mathscr{S}(\mathscr{F}^k X_n)\mathscr{F}^k X_n$$

where $k$ stands for the $k$th power of $\mathscr{F}$. Matrix $\mathscr{F}$ is block-diagonal, and each block $\mathscr{F}_\theta$, $\theta = J, A$, is a regular stochastic matrix. Thus, the Perron–Frobenious Theorem [35] guarantees that the following limit exists

$$\lim_{k\to\infty}\mathscr{F}^k X = \overline{\mathscr{F}}X. \tag{14}$$

Note that the only $N \times N$ stochastic matrix that is not regular is the matrix with all its entries equal to $1/N$. Such a matrix is nilpotent, so that limit (14) trivially holds. Indeed, matrix $\overline{\mathscr{F}}$ is also a block diagonal matrix $\overline{\mathscr{F}} = \mathrm{diag}(\overline{\mathscr{F}_J}, \overline{\mathscr{F}_A})$ such that

$$\overline{\mathscr{F}_\theta} = (\mu_\theta|\cdots|\mu_\theta), \qquad \theta = J, A,$$

where $\mu_\theta = (\mu_1^\theta,...,\mu_N^\theta)$ is the Perron eigenvector, i.e, $\mu_i^\theta$ stands for the asymptotic fraction of individuals of age class $\theta = J, A$ at patch $i = 1, ...,N$. We use limit (14) to build the so called *auxiliary* system (3)

$$\overrightarrow{N}(t+1) = \mathscr{S}(\overline{\mathscr{F}}\overrightarrow{N}(t))\overline{\mathscr{F}}\overrightarrow{N}(t)$$

that approximates the two time scales system (1). In order to perform the dimension reduction, note that

$$\overline{\mathscr{F}} = \begin{pmatrix}\mu_J & \overrightarrow{0}\\ \overrightarrow{0} & \mu_A\end{pmatrix}\begin{pmatrix}\overrightarrow{1}^T & \overrightarrow{0}^T\\ \overrightarrow{0}^T & \overrightarrow{1}^T\end{pmatrix} =: \mathscr{E}\mathscr{G}, \tag{15}$$

where the column vectors $\overrightarrow{1} = (1,...,1)^T$, $\overrightarrow{0} = (0,...,0)^T$ belong to $\mathbb{R}^N$. Note also that the total amount of juveniles or adults remains constant within each reproductive period, that is, it is invariant by the fast dynamics (dispersal). We define the so called *global variables*

$$\mathscr{G}\overrightarrow{N} = \begin{pmatrix}J\\ A\end{pmatrix}$$

(we denote $\overrightarrow{n} = (J, A)^T$) and pre-multiplying system (3) by the $\mathscr{G}$ yields the aggregated system associated to system (1)

$$\overrightarrow{n}(t+1) = \mathscr{G}\mathscr{S}(\mathscr{E}(\overrightarrow{n}(t))\mathscr{E}(\overrightarrow{n}(t) =: \mathscr{L}(\overrightarrow{n}(t))\overrightarrow{n}(t). \tag{16}$$

Once the reduced system is derived, Theorem 2.1 describes the features of the complete system inherited by the reduced system. Theorem 2.1 holds if limits (14) and $\lim_{k\to\infty} D\mathscr{F}^k\overrightarrow{N} = D\overline{\mathscr{F}}\overrightarrow{N}$, where $D$ stands for the differential of $\mathscr{F}$, are uniform on compact sets of $\mathbb{R}^{2N}$, which holds straightforward since $\mathscr{F}$ is linear (for further details, see [34]).

### A2. Derivation of the inherent net reproductive number, the direction of bifurcation, and several proofs

In this section we reproduce known results that can be found in [9,11] to derive the net reproductive number $\overline{\nu}$ given by expression (7) and to write the reduced system (4) in a suitable way to perform the bifurcation analysis.

The Leslie matrix (4) is density-dependent, and we write it as

$$\mathscr{L}(\overrightarrow{N}) = (\mathscr{H}(J, A) + \mathscr{T})\overrightarrow{N}$$

where

$$\mathscr{T} := \begin{pmatrix}0 & 0\\ \overline{\sigma}_J & \overline{\sigma}_A\end{pmatrix} \qquad \mathscr{H}(J, A) := \begin{pmatrix}0 & \overline{\phi}(J, A)\\ 0 & 0\end{pmatrix} \tag{17}$$

and $\mathscr{H}(J, A)$ is rescaled so that $\mathscr{H}(J, A) = \nu\Phi(J, A)$ and $\rho(\Phi(\overrightarrow{0})(I - \mathscr{T})^{-1}) = 1$. The parameter $\overline{\nu}$ is the inherent net reproductive number, and is given by

$\nu = \rho(\mathscr{K}(\vec{0})(I - \mathscr{T})^{-1})$.

Thus, the map defining the dynamics of the aggregated system (4) becomes

$$\mathscr{L}(\vec{N}) = (\nu\Phi(J, A) + \mathscr{T})\vec{N}$$

which depends on the bifurcation parameter $\bar{\nu}$.

For the sake of self-completeness, we recall that the direction of bifurcation is defined [11] as: $\bar{\kappa} = -\vec{w}D\vec{v}$, where $\vec{w}$ and $\vec{v}$ stand, respectively, for the left and right eigenvectors of matrix $\Phi(\vec{0}) + \mathscr{T}(\vec{0})$ associated with the eigenvalue 1. The entry $d_{ij}$ of matrix $D$ is defined by $d_{ij}$: $=\gamma_{ij}^T\vec{v}$, where $\gamma_{ij}$: $=\nabla_x(\phi_{ij}(x) + \tau_{ij}(x))|_{(\nu,x)=(1,0)}$ and $\phi_{ij}, \tau_{ij}$ are the entries of matrices $\Phi$ and $T$, respectively. Direct calculations lead to

$$\bar{\kappa} = -\bar{\sigma}_J\left(\bar{\phi}(\vec{0})\frac{\partial\bar{\phi}(\vec{0})}{\partial J} + \frac{\partial\bar{\phi}(\vec{0})}{\partial A}\right)$$

**Proof of Theorem 3.5.** The proof follows from [11, Theorem 2.1], so that we show that the hypotheses required there are met by system (4). Namely, the entries of matrices $\mathscr{K}$ and $\mathscr{T}$ defined in (17) are of class $C^1$ since the entries of matrix $\bar{s}$ are so (see Section 2). Besides, matrix $(\nu\Phi(\vec{n}) + \mathscr{T}(\vec{n}))$ is primitive for any non-negative $\vec{n} \geq 0$ and $\nu > 0$, $\mathscr{T}(\vec{n}) \neq 0$, $\rho(\mathscr{T}(\vec{n})) < 1$, and $\rho\left(\Phi(\vec{0})(1 - \mathscr{T}(\vec{0}))^{-1}\right) = 1$. □

**Proof of Theorem 3.8.** By assumption, there exists at least one patch with component Allee effect and at least on with none. Therefore, it follows from the definition (13) of $\bar{\kappa}$ that the result holds if we find a dispersal schema (i.e., a regular stochastic matrix) such that its Perron eigenvector gathers a majority of individuals in the above mentioned patch.

Given $\mu = (\mu_1, \ldots, \mu_N) > 0$ such that $\sum\mu_i = 1$, let us choose $a \in (0, 1)$ such that $a\mu_N/\mu_i < 1$ for $i = 1, \ldots, N-1$. Then, the above referred matrix is the matrix $\mathscr{R}$ such that its diagonal elements $r_{ii} = 1 - a\mu_N/\mu_i$, and the sub-diagonal $r_{i+1,i} = a\mu_N/\mu_i$ for $i = 1, \ldots, N-1$. Besides, $r_{1,N} = a$ and all the other entries equal to zero. □

## References


[1] J. Aben, et al., The importance of realistic dispersal models in conservation planning: application of a novel modelling platform to evaluate management scenarios in an afrotropical biodiversity hotspot, J. Appl. Ecol. 53 (2016) 1055–1065.
[2] J. Å ström, T. Pärt, Negative and matrix-dependent effects of dispersal corridors in an experimental metacommunity, Ecology 94 (2013) 72–82.
[3] J. Battin, When good animals love bad habitats: ecological traps and the conservation of animal populations, Conserv. Biol. 18 (2004) 1482–1491.
[4] B. de la Parra R., E. Sánchez, O. Arino, P. Auger, A discrete model with density-dependent fast migration, Math. Biosc.i 157 (1999) 91–109.
[5] B. de la Parra R., M. Marvá, E. Sánchez, L. Sanz, Reduction of discrete dynamical systems with applications to dynamics population models, Math. Models Nat. Phenom. 8 (6) (2013) 107–129.
[6] T. Brochier, et al., Implementation of artificial habitats: inside or outside the marine protected areas? insights from a mathematical approach, Ecol. Modell. 297 (2015) 98–106.
[7] J. Bush, K. Mischaikow, Coarse dynamics for coarse modeling: an example from population biology, Entropy 16 (2014) 3379–3400.
[8] H. Caswell, Perturbation analysis of nonlinear matrix population models, Demogr. Res. 18 (3) (2008) 59–116.
[9] L. Chi-Kwong, H. Schneider, Applications of perron–frobenius theory to population dynamics, J. Math. Biol. 5 (44) (2002) 450–462.
[10] F. Courchamp, L. Berec, J. Gascoigne, Allee Effects in Ecology and Conservation, Oxford University Press, 2008.
[11] J.M. Cushing, Matrix Models and Population Dynamics, Mathematical Biology, in: M. Lewis, A.J. Chaplain, J.P. Keener, P.K. Maini (Eds.), IAS/Park City Mathematics Series, 14 American Mathematical Society, Providence, RI, 2009, pp. 47–150.
[12] J.M. Cushing, Backward bifurcations and strong allee effects in matrix models for the dynamics of structured populations, J. Biol. Dyn. 8 (2014) 57–73.
[13] S. Dey, B. Goswami, A. Joshi, Effects of symmetric and asymmetric dispersal on the dynamics of heterogeneous metapopulations: two-patch systems revisited, J. Theor. Biol. 345 (2014) 52–60.
[14] M.S. Fowler, Density dependent dispersal decisions and the Allee effect, Oikos 118 (2009) 604–614.
[15] D. Franco, A. Ruiz-Herrera, To connect or not to connect isolated patches, J. Theor. Biol. 370 (2015) 72–80.
[16] https://github.com/marcosmarva/DensityDependetFertility_and_IndividualsDispersal.
[17] P.H. Harvey, K. Ralls, Inbreeding, do animals avoid incest? Nature 320 (1980) 575–576.
[18] A. Hastings, L.W. Botsford, Persistence of spatial populations depends on returning home, Proc. Natl. Acad. Sci. USA 103 (2006) 6067–6072.
[19] R.A. Horn, C.R. Robinson, Matrix Analysis, Cambridge University Press, Cambridge, 1985.
[20] R.H. Jongman, D. Kamphorst, Ecological corridors in land use planning and development policies: National approaches for ecological corridors of countries implementing the pan-european landscape and biological diversity strategy. council of europe, 2002.
[21] M.A. LaRue, C.N. Nielsen, Modelling potential dispersal corridors for cougars in mid-western north america using least-cost path methods, Ecol Modell 212 (3–4) (2008) 372–381.
[22] M.A. Leibold, et al., The metacommunity concept: a framework for multi-scale community ecology, Ecol. Lett. 7 (2004) 601–613.
[23] M. Lettink, et al., Removal of introduced predators, but not artificial refuge supplementation, increases skink survival in coastal dune land, Biol. Conserv. 143 (2010) 72–77.
[24] C. Lett, P. Auger, F. Fleury, Effects of asymmetric dispersal and environmental gradients on the stability of host parasitoid systems, Oikos 109 (2005) 603–613.
[25] S.A. Levin, The problem of pattern and scale in ecology, Ecology 73 (1992) 1943–1967.
[26] D. Ludwig, D.D. Jones, C.S. Holling, Qualitative analysis of insect outbreak systems: the spruce budworm and forest, J. Anim. Ecol. 44 (1978) 315–332.
[27] M. Marvá, B. de la Parra R., Coexistence and superior competitor exclusion in the Leslie–Gower competition model with fast dispersal, Ecol. Modell. 306 (24) (2015) 247–256.
[28] M.G. Neubert, H. Caswell, Density-dependent vital rates and their population dynamic consequences, J. Math. Biol. 41 (2) (2000) 103–121.
[29] J.B. Pichancourt, F. Burela, P. Auger, Assessing the effect of habitat fragmentation on population dynamics: an implicit modelling approach, Ecol. Modell. 192 (3–4) (2006) 543–556.
[30] R.C. Team, R: a language and environment for statistical computing, R Foundation for Statistical Computing, Vienna, Austria (2013). http://www.R-project.org/.
[31] C.J. Reading, A proposed standard method for surveying reptiles on dry lowland heath, J. Appl. Ecol. 34 (4) (1997) 1057–1069.
[32] R. Revilla, T. Wiegand, Individual movement behavior, matrix heterogeneity, and the dynamics of spatially structured populations, Proc. Natl. Acad. Sci. USA 105 (2008) 19120–19125.
[33] B.A. Robertson, R.L. Hutto, A framework for understanding ecological traps and an evaluation of existing evidence, Ecology 87 (5) (2006) 1075–1085.
[34] L. Sanz, B. de la Parra R., E. Sánchez, Two time scales non-linear discrete models approximate reduction, J. Differ. Equ. Appl. 14 (6) (2008) 607–627.
[35] E. Seneta, Non-negative Matrices and Markov Chains, second ed., Springer, New York, 1981.
[36] T. Nguyen Huu, P. Auger, C. Lett, M. Marvá, Emergence of global behaviour in a host-parasitoid model with density-dependent dispersal in a chain of patches, Ecol. Complexity 5 (1) (2008) 9–21.
[37] T. Nguyen Huu, B. de la Parra R., P. Auger, Approximate aggregation of linear discrete models with two time-scales: re-scaling slow processes to the fast scale, J. Differ. Equ. Appl. 17 (4) (2011) 621–635.
[38] I. Ugarcovici, H. Weiss, Chaotic dynamics of a nonlinear density-dependent population model, Nonlinearity 17 (2004) 1689–1711.
[39] I. Ugarcovici, H. H. Weiss, Chaotic attractors and physical measures for some density-dependent Leslie population models, Nonlinearity 20 (2007) 2897–2906.
[40] N. Watanuki, B.J. Gonzales, The potential of artificial reefs as fisheries management tools in developing countries, Bull. Mar. Sci. 78 (2006) 9–19.
[41] J. Wolff, What is the role of adults in mammalian juvenile dispersal? Oikos 68 (1) (1993) 173–176.
[42] Y. Xie, Knitr: A Comprehensive Tool for Reproducible Research in R, in: V. Stodden, F. Leisch, R.D. Peng (Eds.), Implementing Reproducible Computational Research, Chapman and Hall/CRC, 2014.
[43] Y.A. Pykh, S.S. Efremova, Equilibrium, stability and chaotic behavior in Leslie matrix models with different density-dependent birth and survival rates, Math. Comput. Simul. 52 (2000) 87–112.